Hydrochemical and isotopic characteristics of geothermal fluids in Tongzhou District, Beijing, and their geothermal significance

YUAN Lijuan, ZHANG Jinping, HE Yuncheng, KONG Xiangjun, GAO Jian
Beijing Geothermal Research Institute, Beijing, 100012

Abstract: Tongzhou, as a sub-center of Beijing city, is rich in geothermal resources and has a huge demand for clean energy for regional construction. This paper aims to grasp the hydrochemical isotopic characteristics of geothermal fluids in the area, understand the recharge, circulation, and thermal storage temperature distribution of the Jixian karst geothermal system, and provide scientific support for the development and protection of geothermal resources in the city. Based on a full understanding of the tectonic and geological conditions in the study area, this paper uses water chemistry and ^{2}H, ^{18}O, ^{3}H, ^{14}C, and n(^{87}Sr)/n(^{86}Sr) isotopic tracers to carry out the work. In the western part of Tongzhou district, within the Daxingdian uplift tectonic unit, the water age increases from northwest (18 ka) to southeast (27 ka) with a transport rate of about 1.5 m/a, and the reservoir temperature increases from 57.4°C to 86.5°C. The Xiadian fracture in the southeast is a hydraulic and thermal conductivity fracture on which the geothermal water age decreases to 8.4 ka, while the reservoir temperature increases to 107.8°C. Both strontium content and strontium isotope values in geothermal water increase along the direction of groundwater runoff, revealing the superimposed effects of two processes: dissolution of strontium in Jixian system carbonates and decay of ^{87}Rb, the latter showing a significant time-accumulation effect, which is more evident in the southeastern part of the study area. The recharge source is atmospheric precipitation in the northwestern or northern mountainous areas of Beijing, with an average recharge elevation of 1510 m. The age and temperature of geothermal water in the thermal reservoir show obvious tectonic control characteristics. Regionally, changes in strontium content and strontium isotope values can effectively trace the transport of geothermal fluids and the degree of

water-rock interaction.

Keywords: Beijing Tongzhou; geothermal fluid; hydrochemistry; strontium isotope; reservoir temperature

The capital city construction has a large demand for geothermal resources. Beijing, as one of the six capitals in the world with geothermal resources, has a large scale of geothermal resource development. At the end of 2019, there are 533 geothermal wells in Beijing, and depths of which are distributed between 2,000 m and 4,000 m. This has made it possible to study geothermal systems in the depth range of 2000 m~4000 m below the surface, and the hydrochemical and water stable isotopic characteristics of geothermal fluids in the Jixian system thermal reservoir in the Beijing plain area are known (Yu Yuan, 2006; Liu Kai et al., 2017; Yuan Lijuan et al., 2020). But the recharge and circulation characteristics of geothermal fluids are less involved. Previous studies have shown that strontium isotopes are sensitive to water-rock interaction and can be used as an effective means to trace groundwater circulation (Zhiyuan Ma and Jijiao Fan, 2005). Strontium is very stable geochemically and does not fractionate during hydrogeochemistry, and different rock components have specific n(87Sr)/n(86Sr) values, resulting in different water bodies may have different n(87Sr)/n(86Sr) values and correspond to different geological environments (Ye et al, 2008). Tracer studies of strontium elements and strontium isotopes in geothermal fluids have not been carried out in Beijing, and the effects of their application in geothermal systems are not known.

As a sub-center of Beijing, Tongzhou is the largest construction project in Beijing during the 14th Five-Year Plan period, and the regional construction has a huge demand for clean energy. The exploration breakthrough of medium-temperature geothermal resources in eastern Tongzhou in 2015 has greatly promoted the development of geothermal resources in Tongzhou (Zou Dengliang et al., 2015). The geothermal water recharge and circulation, as well as the distribution of thermal storage temperature, is the basis for the scientific and reasonable development of geothermal resources. In this paper, we systematically describe the hydrochemical

isotopic characteristics of geothermal fluids in Tongzhou district by means of water chemistry and isotopes such as 2H, 18O, 3H, 14C, and n(87Sr)/n(86Sr), focusing on the characteristics of recharge sources, circulation, and thermal storage temperatures of geothermal fluids in the thermal reservoir of the Jixian system in the Middle Met sedimentary, hoping to provide scientific support for the development and protection of urban geothermal resources.

1 Overview of Tongzhou District

Tongzhou District is located in the southeastern part of the Beijing Plain, with a total area of 906 km2. The topography of the district is flat, with a general inclination from northwest to southeast. The annual average temperature is 11.3℃ and the precipitation is about 620 mm.

The Nanyuan-Tongxian Fault and the Xia Dian Fault in the north-east direction divide the study area into three Class III tectonic units: the Beijing Iteration Fault (III6), the Daxing Iteration Uplift (III7) and the Dazhan New Fault (III8) (Figure 1). The Daxing Uplift has the largest area, and two groups of north-east-south-west fractures and north-west-south-east fractures intersect in this tectonic unit, forming a hydraulic and thermal conductivity channel. The stratigraphy in the area is developed from old to new, including the Taikoo, Yuangu, Jixian and Baikou systems, the Paleozoic Cambrian, Ordovician, Carboniferous and Permian systems, and the Cenozoic Paleocene, Neoproterozoic and Quaternary systems (Beijing Municipal Bureau of Geology and Mines, 1982).

The dolomite of the Jixian System Wuzhishan Formation is the main thermal reservoir within the Tongzhou District, dominated by smectite dolomite with more developed flint bands. The main mineral is dolomite, with the content of 72.8%~98.9%, followed by quartz and feldspar, with the content of 1%~20% (Kong Xiangjun, 2019). The thermal reservoir of the Jixian System Wushan Formation is distributed throughout the region, and the complete thickness of the formation is about 2230 m (Beijing Bureau of Geology and Mines, 1982). Available borehole data

show that the burial depth of thermal reservoirs in the eastern Beijing Di Di Fault (III6) is 500 m~800 m; the shallowest burial depth of thermal reservoirs in the central Daxing Di Uplift (III7) is 474 m and the maximum is about 2500 m; and the minimum burial depth of thermal reservoirs in the southeastern Dafang New Fault (III8) is about 2500 m and the maximum is over 5000 m. The scale of geothermal resource development and utilization in Tongzhou District is large, and up to now, 29 geothermal wells have been completed, most of which are located within the Daxingdian uplift (Figure 1). The maximum drilling depth of the current geothermal wells in the district is 3588.88 m, and the highest water output temperature is 91°C. The well is located on the Xia Dian Fault. The currently discovered geothermal wells in Beijing with water output temperatures higher than 90°C are located along the Xia Dian Fault and its extensions (Zhang Jinping and Yuan Lijuan, 2015).

2 Data sources

Twenty-three pieces of geothermal water were collected between 2015 and 2019 from the Jixian System Misty Mountain Formation aquifer in the region (Table 1). In order to grasp the circulation characteristics of geothermal fluids, 6 pieces of atmospheric precipitation, 8 pieces of surface water and 36 pieces of Quaternary groundwater were also collected, totaling 73 water samples (Fig. 1). The main test items include water chemistry, 3H, δD, δ18O, 14C and n(87Sr)/n(86Sr). Geothermal full analysis tests were completed at the Beijing Hydrogeology and Engineering Geology Brigade. To ensure the representativeness of the samples, water chemistry test samples were collected using dry polyethylene bottles with a volume of 10 L that had been cleaned by a prescribed procedure, then sealed with threaded caps and delivered to the laboratory within 24 h to complete the analysis tests with a relative error of <±5% for anion and cation balance checks. The analysis of the other water samples for the main trace element test, as well as the tritium content and n(87Sr)/n(86Sr) tests of all water samples were done at the Analysis and Testing Research Center of the Beijing Institute of Nuclear Industry. 3H tests were done with

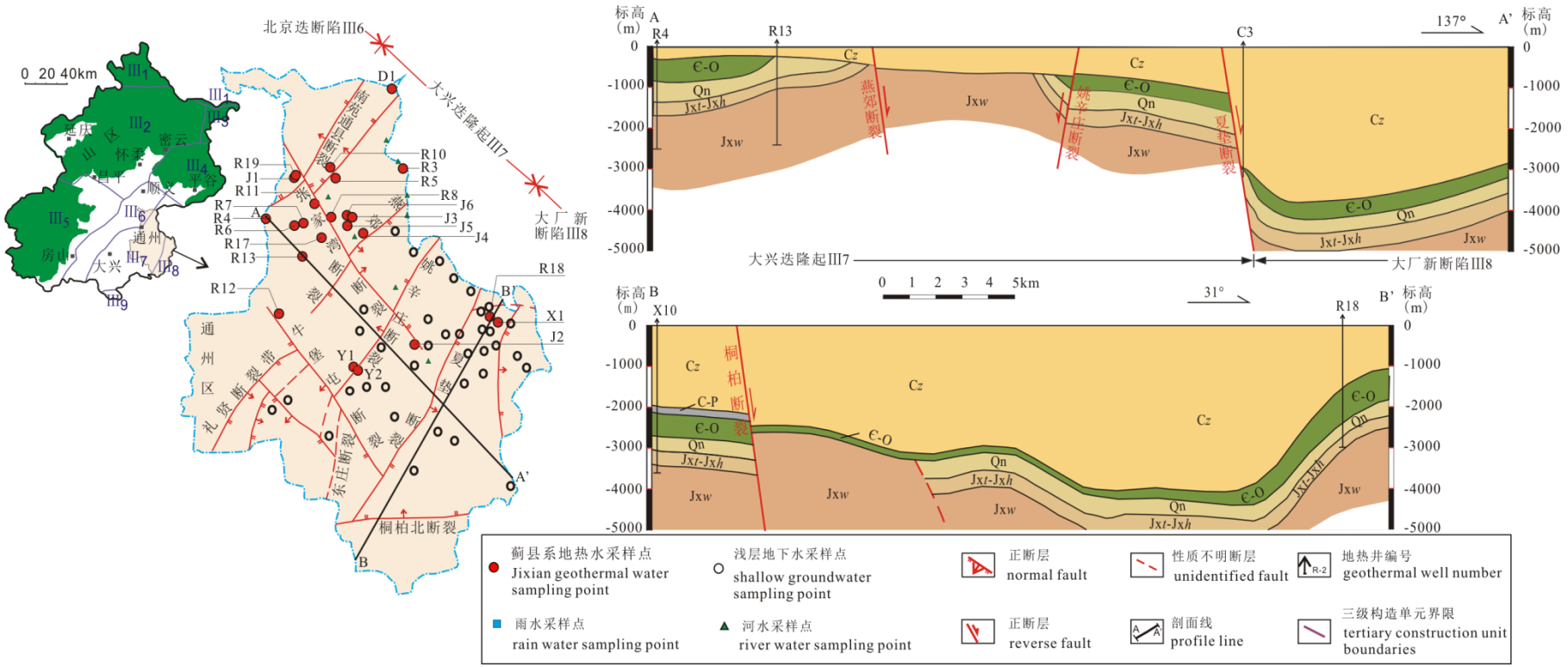

Fig.1 Distribution of sampling sites and geological profiles in Tongzhou District, Beijing

Table 1 Hydrochemical and isotpic data of the hydrothermal fluid in Tongzhou area, Beijing

No	Temp°C	pH	$\delta^{18}O$	δD	^{3}H	^{14}C	$\delta^{13}C$	$n(^{87}Sr)/n(^{86}Sr)$	Sr^{2+}	H_2SiO_3	Na^+	K^+	Ca^{2+}	Mg^{2+}	Cl^-	F^-	SO_4^{2-}	HCO_3^-	CO_3^-	TDS
			(VSMOW,‰)		（TU）	(pMC)	（VPDB,‰）		（mg/L）											
T3	42	8.1	/	/	/	/	/	/	0.102	26.8	127.0	6.1	11.0	9.0	45.2	10.4	29.8	248.0	6.0	355.1
T4	58	8.3	-10.8	-79.77	/	2.89	-5.6	0.7090	0.320	32.0	155.0	7.2	17.2	8.6	75.0	7.8	69.2	229.0	14.4	454.0
T5	46	8.3	-11.2	-81.52	/	2.34	-7.6	0.7096	0.160	27.2	131.0	4.1	10.4	4.9	51.8	9.0	19.1	251.0	8.4	351.0
T6	51	8.5	-11.2	-81.99	/	/	/	0.7107	0.190	24.0	127.0	5.3	10.4	6.2	54.9	7.8	15.9	226.0	26.4	345.9
T7	49	8.4	-11.2	-81.67	<1.3	3.42	-5.8	0.7094	0.200	25.4	124.0	5.3	11.0	6.9	50.9	7.7	30.3	243.0	18.0	359.0
T8	53	7.9	/	/	/	/	/	/	0.130	37.0	206.0	22.4	12.0	19.4	60.0	30.0	4.7	531.0	0.0	590.0
T10	48	8.0	/	/	/	/	/	/	0.173	30.4	120.0	3.7	18.0	8.5	54.5	8.0	35.7	283.0	0.0	381.9
T11	45	8.1	/	/	/	/	/	/	0.144	30.0	127.0	3.3	13.6	6.4	40.4	6.9	50.7	262.0	6.0	375.4
T12	41	7.9	-11.0	-80.80	/	2.26	-8.6	0.7103	0.260	25.1	127.0	14.6	17.0	13.7	57.7	11.4	86.7	245.0	0.0	439.2
T13	48	9.1	-11.0	-80.96	/	/	/	0.7118	0.200	27.2	205.0	17.6	6.6	4.6	60.7	16.3	14.8	330.0	48.0	498.3
T17	35	8.7	-10.6	-78.70	<1.3	/	/	/	0.141	38.5	229.0	22.1	6.0	5.6	66.1	18.8	51.8	367.0	30.0	579.1
T18	55	8.0	-9.1	-75.23	<1.3	2.00	-8.2	/	0.537	99.4	492.0	21.8	34.1	11.4	401.0	9.3	16.4	734.7	0.0	1344.1
T19	43	8.3	-11.3	-83.19	/	/	/	0.7087	0.170	25.8	138.0	3.6	11.9	4.7	44.2	6.9	55.2	221.0	14.4	375.3
J1	41	8.4	-11.4	-83.45	/	5.08	-7.1	0.7088	0.170	24.6	137.0	3.5	11.3	4.3	45.1	7.0	55.7	228.0	10.8	376.3
J2	54	8.8	-10.4	-77.98	<1.3	1.40	-8.5	0.7133	0.319	38.4	330.0	22.4	4.2	3.6	165.0	8.8	0.8	522.0	55.2	814.6
J3	52	8.1	-10.4	-76.10	<1.3	0.80	-5.4	/	0.397	32.5	169.0	25.1	6.0	14.8	57.7	17.9	20.3	358.0	13.2	478.5
J4	46	7.2	-9.2	-73.20	<1.3	2.00	-5.7	/	0.250	34.8	184.0	26.1	36.7	36.6	159.0	16.2	91.0	428.0	0.0	747.4
J5	51	7.7	/	/	/	/	/	/	0.140	33.0	137.0	18.1	11.6	15.8	66.7	15.4	11.9	354.0	0.0	438.1
J6	54	7.8	/	/	/	/	/	/	0.200	12.1	148.0	24.5	9.0	13.4	59.9	15.7	31.1	356.0	0.0	463.9
X1	91	7.6	-9.6	-78.45	<1.3	3.45	-2.2	0.7145	0.590	72.2	524.0	54.6	13.7	6.6	282.0	17.1	55.3	943.0	0.0	1407.7
D1	38	9.6	-11.2	-82.05	/	2.33	-4.9	0.7102	0.040	6.5	119.0	2.0	3.8	2.2	44.9	7.0	2.8	94.0	75.6	259.6
Y1	38	8.1	-10.5	-79.58	/	/	/	0.7130	0.220	20.0	242.0	11.9	8.0	5.2	98.3	13.1	61.1	381.0	19.2	626.6
Y2	45	7.8	-10.5	-78.52	/	1.09	-5.6	0.7153	0.320	30.2	213.0	12.9	14.5	9.9	132.0	11.4	2.8	430.0	0.0	600.1

a Quantulus 1220-003 low background liquid flash meter with a detection limit of 1.3 TU. n(87Sr)/n(86Sr) was measured using a The absolute deviations of the 23 samples in this batch were in the range of 0.000010~0.000025. δD, δ18O, δ14C and δ13C were entrusted to the BETA laboratory and completed by isotope ratio mass spectrometry and gas pedal mass spectrometry, respectively.±1 ‰, ±0.2 pMC and ±0.3 ‰, respectively.

3 Results and discussion

3.1 Hydrochemistry, isotope characteristics and recharge sources

The anions in different water bodies in the study area were all dominated by HCO3-, and the cation composition varied widely (Figure 2). The temperature distribution of geothermal water in the area was in the range of 35°C ~91°C, the pH distribution was in the range of 7.2~9.6, the TDS distribution was in the range of 309 mg/L~1409 mg/L with the average value of 536 mg/L, and the geothermal water chemistry type was of HCO3--Na+ type. The TDS of the fourth series groundwater was distributed in the range of 310 mg/L~447 mg/L with a mean value of 364 mg/L. According to the Shukarev classification, the water chemistry type included HCO3--Na+ type and HCO3--Ca2+-Na+ type. The TDS of rainwater was distributed in the range of 19 mg/L to 73 mg/L. The high SO42- content in some of the rainwater samples may be the contribution of SO2 from coal combustion (Aas et al., 2007; Xu Zhifang and Han Guilin, 2009). The TDS of river water was distributed in the range of 351 mg/L to 646 mg/L. There was a certain degree of Cl- enrichment, which exhibited the water chemistry process of evaporative concentration.

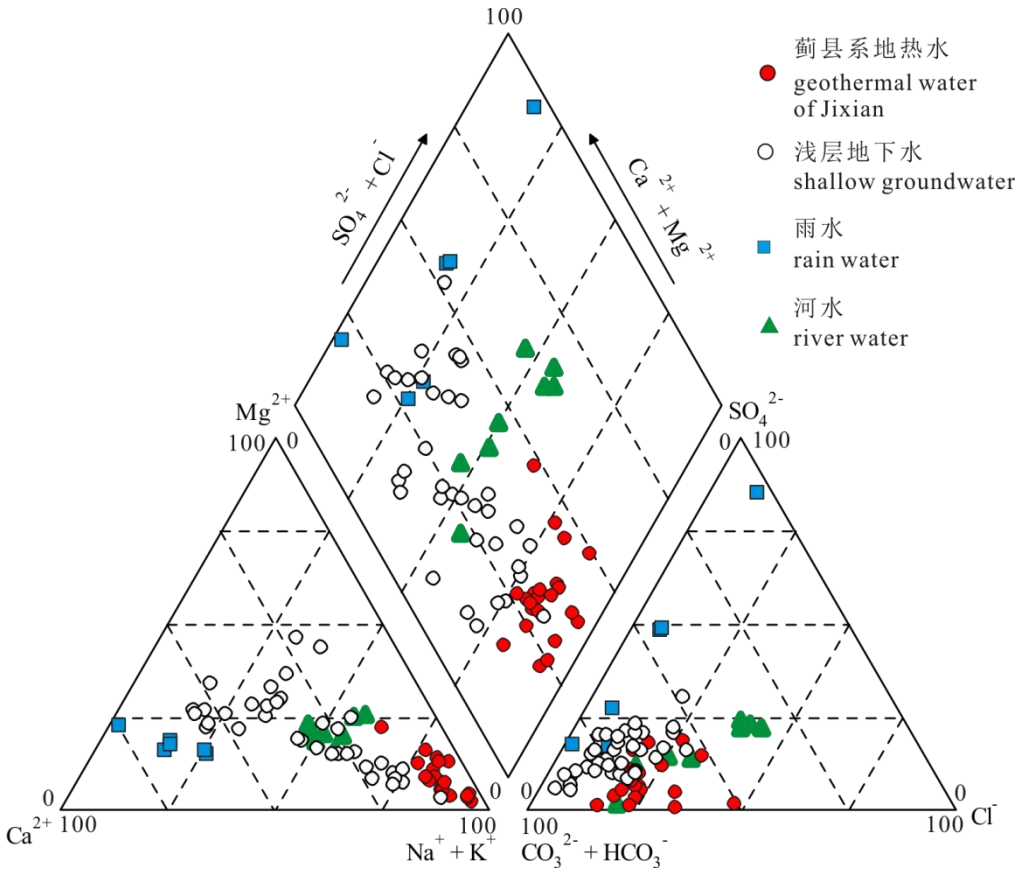

Fig.2 Piper diagram of the water samples in Tongzhou (the unit of the ions in figures is milligram equivalent percent)

The δ18O and δD compositions of different water bodies in the study area are shown in Fig. 3. Both the fourth-series groundwater in Tongzhou district and the Jixian-series geothermal water point down to the right of the local atmospheric precipitation line (Li Jie et al., 2018) and are almost parallel to it. The same phenomenon occurs in Beijing soil water (Deng Wenping et al., 2013) and Yanqing basin groundwater (Li Jie et al., 2018). The reason for this phenomenon is that rainfall enters the soil and mixes with evaporation-influenced groundwater in the soil, causing the isotopic composition of groundwater to deviate from the local atmospheric precipitation line (Allison et al., 1984).

The δ18OV-SMOW of the Quaternary groundwater was scattered in the range of -11.7‰ to -6.4‰. Compared with the isotopic composition of the Quaternary groundwater, the δ18OV-SMOW composition of geothermal water is more concentrated, with a distribution range of -11.4‰ to -9.1‰ and a mean value of

-10.5‰. Combined with the water chemistry composition characteristics (Figure 3), an interesting phenomenon emerges: when the Quaternary groundwater is enriched in δ18O V-SMOW (-9.0‰ to -7.0‰), its milligram equivalent percentage of Ca2+ (the percentage of milligram equivalents of this ion to the total milligram equivalents of anions or cations) is high (mean value of about 46%), Na+ concentration is low (mean value of about 28%), and groundwater chemistry type The groundwater chemistry type is HCO3--Ca2+-Na+ type. In contrast, when the isotopic composition (δ18O V-SMOW <-9.0‰) of the Quaternary groundwater is similar to that of geothermal water, the average value of Ca2+ concentration in Quaternary groundwater decreases to 24%, while the average value of Na+ concentration increases to nearly 68%, and the groundwater chemistry is of HCO3--Na+ type.

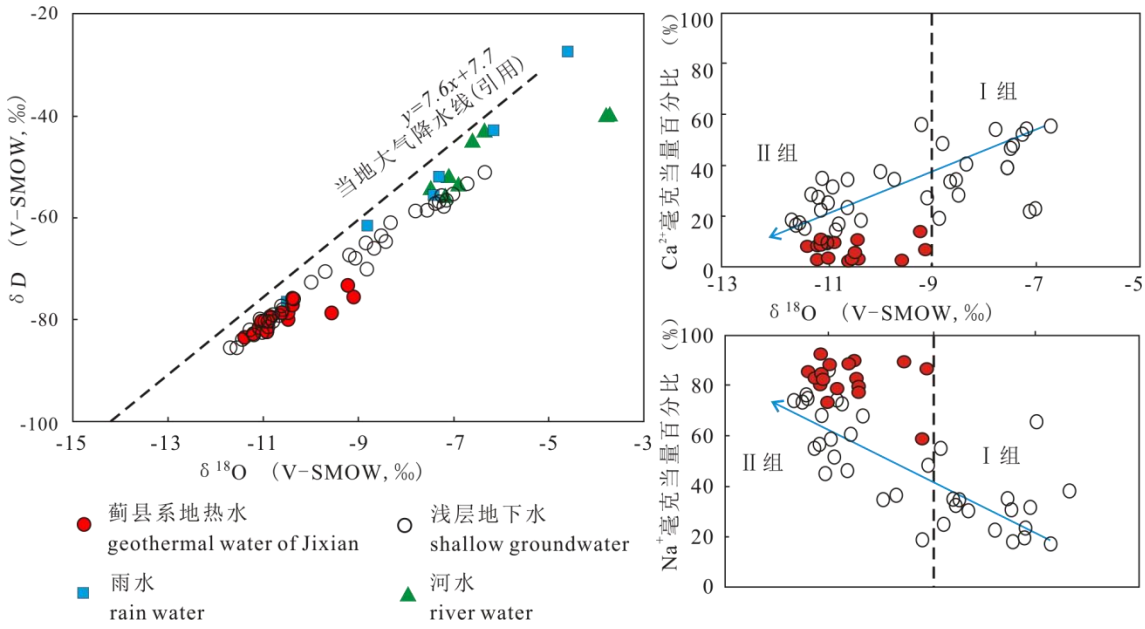

Fig. 3 Relationship between $\delta^{18}O_{V\text{-}SWOM}$ and $\delta D_{V\text{-}SWOM}$ of water samples in Tongzhou

This change coincides with the chemical evolution of freshwater in the North China Plain region: along with the increase in circulation paths, circulation time, and enhanced dissolved filtration, the water chemistry type shifts from HCO3---Ca2+ to HCO3---Ca2+-Na+ and then to HCO3-- -Na+ (Guo, Y. H. et al., 2002). Group Ⅰ originates from the vertical infiltration recharge of local atmospheric precipitation, and the oxygen isotopes are closer to the mean value of local atmospheric precipitation, with a short circulation path and a low degree of dissolution and filtration. The increase of absolute and relative Na+ content in the groundwater of

Group II indicates that it has experienced a higher degree of dissolution and filtration, and is more similar to the geothermal water chemistry of the Jixian system. Combining with the hydrogeological conditions, the loose pore space aquifers of the Quaternary in the eastern and western parts of Tongzhou District are the front edge of the Chaobai River-Jianyun River-Wenyu River alluvial fan and Yongding River alluvial fan, respectively, and the recharge source of Group II may be the lateral runoff recharge from the mountainous areas in the north and northwest (Beijing Municipal Bureau of Geological and Mineral Exploration and Development and Beijing Municipal Hydrogeology and Engineering Geology Brigade, 2008).

The revealed elevation effect in the geothermal water recharge process can be calculated using the groundwater recharge elevation calculation formula.

$$H = \frac{\delta^{18}O_r - \delta^{18}O_a}{grad^{18}O_r} + h \quad \text{……（1）}$$

In the above equation: H is the recharge elevation; δ18Or is the stable isotopic composition of atmospheric precipitation at the recharge elevation, and the average value of δ18O of geothermal water is taken as -10.5 ‰; δ18Oa is the average composition of local atmospheric precipitation, and it is taken as -7.5 ‰; h is the average local ground elevation, and it is taken as the average ground elevation of Tongzhou District, 10 m; grad18Or is the gradient value of δ18O of precipitation with elevation in the basin, and it is taken as grad18Or is the gradient of precipitation δ18O with elevation in the basin, which is taken as -0.2 ‰/100 m (Liu Jianrong et al., 2009). It is known that the recharge elevation is 1510 m. Combining with the regional hydrogeological conditions, it can be assumed that the source of geothermal water recharge in Tongzhou District is the mountainous area above 1510 m in the northwest and Beijing.

3.2 Groundwater age and circulation route

3.2.1 Groundwater age

In this paper, we use 3H and 14C isotope techniques to determine the age of

geothermal water, and the results show that the 3H content in geothermal water is below the detection limit in all cases and the 14C content is less than 5.08 pMC.

14C dating is based on the measurement of the decrease of the parent radionuclide (14C) in a given sample. In essence, groundwater 14C dating is not a determination of the age of the water, but of the age of dissolved inorganic carbon in groundwater. Assumptions: groundwater contains the radioisotope 14C, and once it enters the groundwater system and its 14C is not newly replenished, 14C begins to decay according to the decay law, and groundwater dating can be based on the decay equation.

$$t = \frac{1}{\lambda} \ln \frac{A_0}{A_t} = 8267 \ln \frac{A_0}{A_t} \qquad (2)$$

Where: t is the apparent age of groundwater (a); λ = 12.1×10-6/a, which is the 14C decay constant; A0 is the initial radioactivity concentration (pMC) of the parent nucleus, which is taken as 100 pMC (Clark and Fritz, 1997); At is the radioactivity concentration (pMC) of the sample 14C.

If the 14C from soil CO2 has been preserved in the groundwater during the flow process and has not been diluted, then equation (2) can be used to determine the age, but the geothermal water reservoir in Tongzhou District is a carbonate formation, and carbonate minerals are mostly formed during the geological history, and their 14C concentration is generally close to 0 pMC. Under the influence of water-rock interaction, the dissolution of carbonate minerals from aqueous media into groundwater will reduce the 14C concentration in groundwater, which is called "dilution reaction". To correct for the effect of carbonate thermal reservoirs on 14C dating of geothermal water, a dilution factor q was calculated using the Pearson isotope δ13C mixing model (1965), taking into account the addition of 14C radioactive DIC during carbonate dissolution in open system conditions and the subsequent 14C dilution in closed system conditions.

$$q = \frac{\delta^{13}C_{DIC} - \delta^{13}C_{card}}{\delta^{13}C_{soil} - \delta^{13}C_{card}} \qquad (3)$$

Where: δ13CDIC is the 13C measurement of groundwater; δ13C soil is the δ13C

of soil CO2 (usually close to -23 ‰); and δ13Ccard is the δ13C of dissolved calcite (usually close to 0 ‰).

After dilution correction, the decay equation for groundwater dating becomes.

$$t = \frac{1}{\lambda} \ln \frac{q \times A_0}{A_t} = 8267 \ln \frac{q \times A_0}{A_t} \quad (4)$$

Table 2 ^{14}C corrected model age of geothermal water in Tongzhou

No	Well depth（m）	Apparent age（ka）	Pearson Model corrected age（ka）
T4	2501	29	18
T5	2679	31	22
T7	2203	28	17
T12	2405	31	23
T18	3203	32	24
J1	2507	25	15
J2	2800	35	27
J4	2801	32	21
X1	3589	28	8.4
D1	2109	31	18
Y2	2502	37	26

The 14C-corrected model ages of geothermal water in the study area are shown in Table 2. The corrected ages of geothermal water in the area are distributed in the range of 8.4 ka to 27 ka, indicating that geothermal water in the area belongs to the old water cycle with poor renewal ability. The apparent ages of J-1 well in the northwest and Y-2 well in the southeast are 18 ka and 27 ka, respectively, and the transport rate of hot water in the Jixian system thermal reservoir between J-1 well and Y-2 well is about 1.5 m/a in the A-A' section. The apparent age of groundwater in well X-1, where the summer pad fracture was encountered, is only 8.4 ka.

3.2.2 Sr isotope in geothermal water system

The Sr2+ concentration in groundwater depends on the Sr content in the water-bearing medium and the degree of water-rock interaction (Shand, 2009; Zhai, Yuanzheng et al., 2011). The average Sr2+ concentration in atmospheric precipitation in the study area was 0.008 mg/L. The Sr2+ concentrations in geothermal fluids and

Quaternary groundwater ranged from 0.040 mg/L to 0.590 mg/L and 0.195 mg/L to 0.551 mg/L, respectively, with mean values of 0.230 mg/L and 0.339 mg/L. Sr in nature cannot exist in Sr in nature does not exist in monomeric form, but mainly in homogeneous form. Strontium and calcium belong to the same main group in the periodic table and are in close proximity to each other. Sr is often found in a dispersed state in calcium-bearing minerals, such as carbonates, apatite, hornblende and plagioclase. Due to the geochemical affinity of Sr and Ca, they are often considered to exhibit consistent geochemical behavior in geochemical studies (Shand et al., 2009). The variability of Sr2+ concentration in groundwater in Tongzhou area is much smaller than that of Ca2+, but Sr2+ and Ca2+ are both largely positively correlated (Figure 4), indicating that Sr and Ca in water undergo roughly similar hydrogeochemistry after precipitation enters the water-bearing medium. Compared with the Quaternary groundwater, Sr2+ in geothermal water also increased along with Ca2+, but the rate of Sr2+ increase was greater.

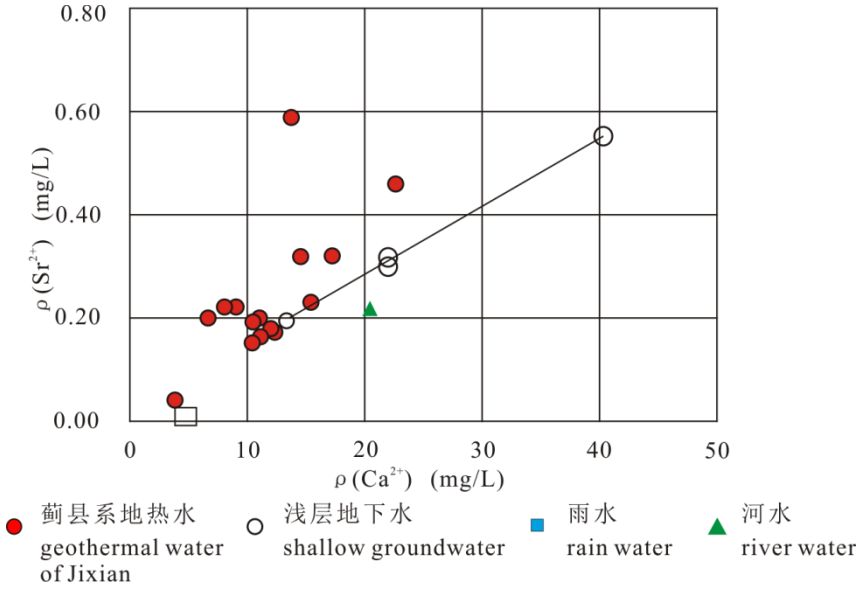

Fig.4 Sr^{2+} versus Ca^{2+} in water samples in Tongzhou

The n(87Sr)/n(86Sr) values in geothermal water were distributed in the range of 0.7087 to 0.7153. In contrast, the variability of n(87Sr)/n(86Sr) values in atmospheric precipitation (0.7107-0.7115), river water (0.7100) and Quaternary groundwater (0.7092-0.7097) in the study area are all smaller, probably due to the single source of Sr elements in these water bodies or the different water-rock interactions experienced

by geothermal water. Airborne dust (n(87Sr)/n(86Sr) value of 0.7111) is an important source of strontium in atmospheric precipitation in Beijing (Xu Zhifang and Han Guilin, 2009). The sources of strontium in groundwater mainly include wind-sourced sediments, weathering release products of minerals such as silicates, carbonates or sulfates in soils, and aqueous media. The n(87Sr)/n(86Sr) values of strontium from carbonate and sulfate sources are about 0.7080, and the n(87Sr)/n(86Sr) values of strontium from silicate sources are generally 0.7160-0.7200 (Gaillar et al., 1999; Philippe, 2006; Min Maozhong et al., 2007). . The n(87Sr)/n(86Sr) values in the Quaternary groundwater of Tongzhou district are similar to the n(87Sr)/n(86Sr) ratios of the weathering source of carbonate rocks, and the strontium in groundwater may originate from the dissolution of strontium elements in carbonate rocks. The n(87Sr)/n(86Sr) values in geothermal water fall between the strontium isotopic compositions of carbonate rocks and silicate mineral sources, and the strontium isotopic compositions are closer to the n(87Sr)/n(86Sr) values of strontium from silicate mineral sources when the Sr2+ content is higher (Fig. 5a). However, the high dolomite content and only a small amount of quartz and calcite in the thermal reservoir of the Jixian System Wushan Formation in the study area (Kong, Xiangjun, 2019), and the dissolution of carbonate rocks should be the main source of strontium in geothermal water in this area from the analysis of the composition of aquifer media.

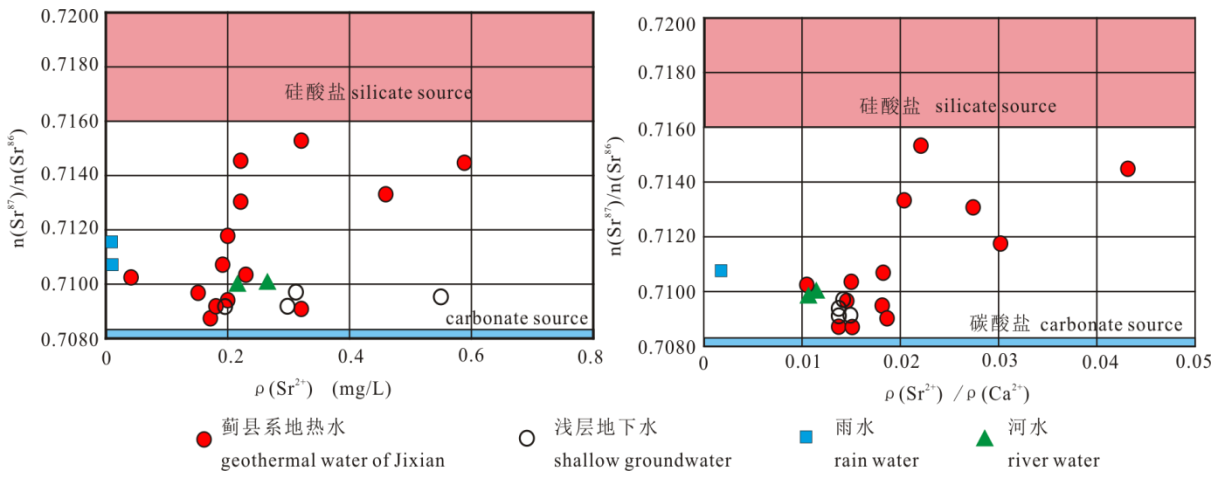

Fig.5 $n(^{87}Sr)/n(^{86}Sr)$ versus$\rho(Sr^{2+})$(a) and $n(^{87}Sr)/n(^{86}Sr)$ vs.$\rho(Sr^{2+})\rho(Ca^{2+})$(b) in water samples in Tongzhou

The Sr2+/Ca2+Vs87Sr/86Sr relationship demonstrates more clearly the enrichment process of strontium isotopes in geothermal water (Figure 5b). When the geothermal water Sr2+/Ca2+ ratio is small (0.01-0.02), the n(87Sr)/n(86Sr) values (0.7087-0.7107) are close to the n(87Sr)/n(86Sr) values (0.7080) for carbonate sources. And the n(87Sr)/n(86Sr) values increase significantly (0.7118 to 0.7153) for higher Sr2+/Ca2+ values (>0.02). And the distribution of both showed some geographical differences, with the former samples all located in the northwest of Tongzhou District, while the latter were all distributed in the southeast of Tongzhou District. Combined with the groundwater flow field in the study area, it is inferred that the high strontium values may be caused by the time-accumulation effect of strontium. Previous studies have shown that among the four stable isotopes of Sr in nature (88Sr, 87Sr, 86Sr, 84Sr), only 87Sr is of radioactive origin and can be derived from 87Rb through β-decay, and with the decay of Rb, the content of 87Sr can increase continuously as a function of time in rocks and minerals containing Rb, exhibiting a time-accumulation effect.

According to this feature the author et al. plotted the planar distribution of Sr2+ content and n(87Sr)/n(86Sr) (Fig. 6), and both showed a consistent trend of increasing from northwest to southeast (Fig. 6a, b), while the 14C apparent age in the region also showed the same distribution pattern (Fig. 6c). The same distribution pattern of the three reveals the evolution pattern of strontium in geothermal water: on the one hand, along the direction of groundwater flow, the increasing intensity of water-rock reaction leads to the increase of Sr2+ content in geothermal fluid; in addition, with the prolongation of groundwater retention time, the time-accumulation effect leads to the increase of n(87Sr)/n(86Sr) values in geothermal fluid.

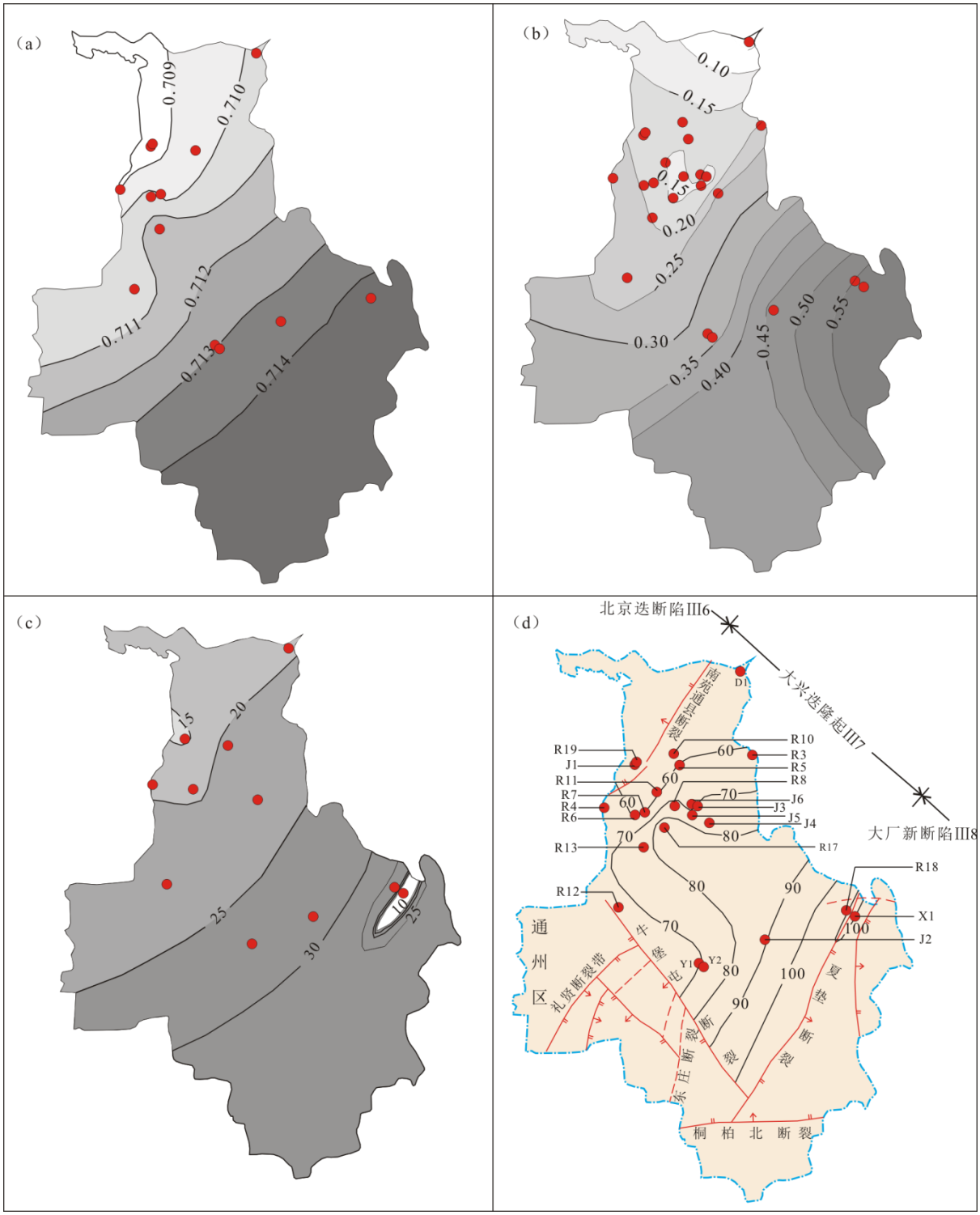

Fig.6 Distribution contour map of $n(^{87}Sr)/n(^{86}Sr)$ (a)、$\rho(Sr^{2+})$(mg/L) (b)、^{14}C corrected model age (ka BP) (c) and thermal storage temperature(℃)(d) in water samples in Tongzhou

3.3 Geothermometer and reservoir temperature

Geothermometer methods are used to directly estimate the temperature of deep thermal reservoirs by using the content of certain chemical components in the underground hot water or the relationship between isotopic values and temperature. There are four major types of geothermometers in common use, namely cationic geothermometers, SiO2 geothermometers, gas geothermometers, and isotope geothermometers, with different application conditions (Fournier, 1997). In this paper, we mainly use cationic geothermometers and SiO2 geothermometers to calculate the thermal storage temperature in the study area. The calculation results show that the estimation results of Na+/K+ and Na+-K+-Ca2+ cation geothermometers with different calculation methods are high, and the estimation results of chalcedony geothermometers are low (Table 2). In addition, most of the geothermal wells in Tongzhou area have discharge temperatures below 100°C, and SiO2 geothermometers with sufficient steam loss are not suitable for evaluating thermal storage temperatures. K+/Mg2+ cationic geothermometers and SiO2 geothermometers without steam loss are more suitable for evaluating thermal storage temperatures in Tongzhou area thermal reservoirs (Table 2). In this paper, the calculation results of K+/Mg2+ cation geothermometer and SiO2 geothermometer without vapor loss are used as reference, and the average value is taken as the thermal storage temperature, then the thermal storage temperature in the study area is distributed in the range of 34°C to 112°C, and the average value is 50°C.

The two wells with thermal storage temperatures over 100° C are located on the Xia mat fracture, the dividing line between the Daxingdian uplift (Ⅲ7) and the Dafangxin fault (Ⅲ8). The remaining geothermal wells are located within the Daxingdian uplift (III7), excluding one anomaly (D1), as its estimated thermal storage temperature is lower than the effluent temperature and the measured temperature at the bottom of the well, and the thermal storage temperature is distributed within 57.4°C~89.6°C, with an average temperature of 68.3°C. Within the Daxingdian uplift (III7), the vertical upward thermal storage temperature does not show a trend of

increasing with the average depth of the reservoir (Figure 7). The average depth of thermal storage in the northwestern part of the Daxingdian uplift (III7) is larger (2534 m~2983 m), but the thermal storage temperature is lower (57.4°C~66.6°C), with an average value of 59.9°C (Figure 7). In the southeastern part of the Daxingdi Uplift (III7), the thermal reservoir becomes shallower (2145 m~2260 m), but the thermal reservoir temperature increases (61.2°C~86.5°C), with a mean value of 72.4°C. The author et al. plotted the thermal reservoir temperature plan according to this feature (Figure 6d), which more visually shows the increasing trend of thermal reservoir temperature from northwest to southeast. The possible reason for this phenomenon is that within the same reservoir, along the direction of groundwater flow, the retention time of the geothermal fluid increases and the heat exchange with the rock is more adequate, which in turn leads to an increase in the thermal storage temperature.

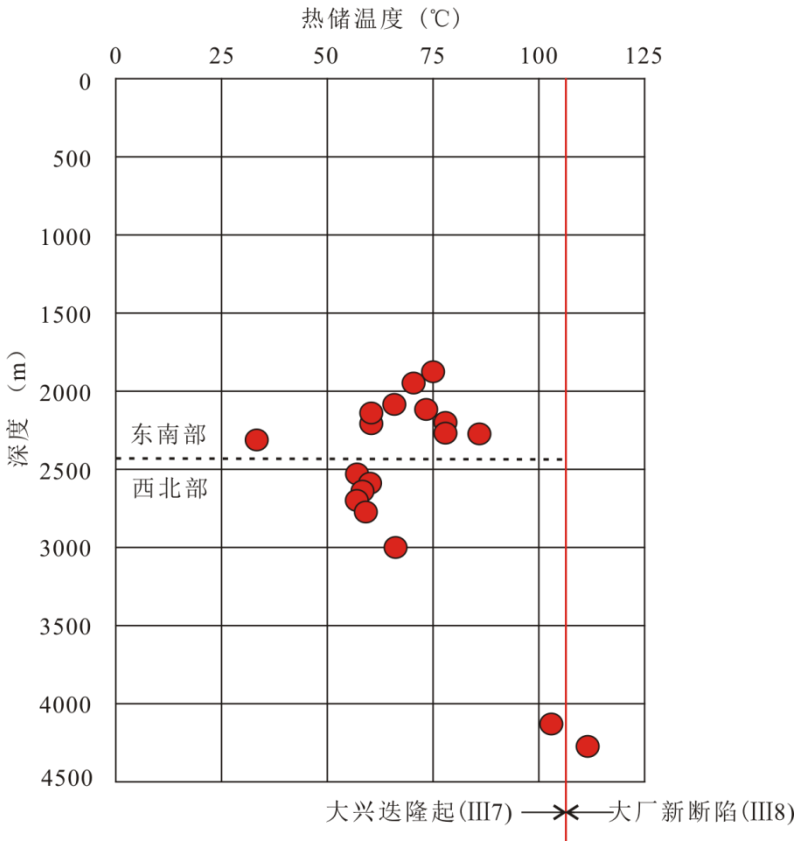

Fig.7 Reservoir temperature with depth

Table 3 Results of reservoir temperature in Tongzhou by different geothermometer（units：℃）

No	Well depth（m）	Temp(℃)	Well testing		reservoir temperature estimation(℃)								
					Cationic geothermometer					SiO2 geothermometer			estimated value
			depth（m）	Temp（℃）	Na/K	Na/K	Na/K	Na-K-Ca	K/Mg	chalcedony	Sufficient steam loss	No steam loss	
R3	1827	42	1800	43	161.7	180.3	131	99.4	57.7	32.6	70	64.6	61.2
R4	2501	58	2417	63	159.4	178.1	128.4	96.9	61.8	39.7	76	71.4	66.6
R5	2679	43	2679	57	133.6	153.4	99.8	86.4	55.4	33.1	70.5	65.1	60.3
R6	2213	51	2210	53	152	171	120.1	95.4	58.6	28.3	66.3	60.5	59.6
R7	2203	49	2200	54	154	173	122.4	94	57.5	30.5	68.2	62.6	60.1
R8	2699	53	2670	57	224.3	239.1	203.7	193.6	78.6	45.8	81.2	77.2	77.9
R10	2509	48	2460	53	133.3	153.1	99.5	70.5	47.7	37.6	74.3	69.4	58.6
R11	2480	45	2450	56	122.8	142.9	88	73	48.1	37.1	73.8	68.9	58.5
R12	2405	41	2350	45	229.2	243.7	209.7	184.4	72.5	30	67.8	62.1	67.3
R13	2401	48	2400	52	204.2	220.4	179.9	185.7	90.7	33.1	70.5	65.1	77.9
R17	2468	35	2460	58	214	229.5	191.4	195.4	94.1	47.5	82.6	78.9	86.5
R18	3203	55	3200	84	155.9	174.7	124.5	152.6	84.5	94.6	120.5	122.7	103.6
R19	2370	43	/	/	124	144.1	89.3	80.2	53.4	31.1	68.7	63.2	58.3
J1	2507	41	2500	55	121.9	142.1	87	79.7	53.4	29.2	67.1	61.4	57.4
J2	2800	54	2800	64	185.9	203.2	158.5	185.7	100.4	47.4	82.5	78.8	89.6
J3	3001	52	3000	63	253.4	266	239.1	215.3	84.8	40.3	76.6	72	78.4
J4	2801	46	2800	54	248.9	261.8	233.6	196	74.6	43.2	79	74.8	74.7
J5	2806	51	2800	57	242.1	255.6	225.2	197.3	75.9	41	77.1	72.6	74.3
J6	3002	54	3000	59	264.4	276	252.8	215.1	85.4	4.2	45.2	37	61.2
X1	3589	91	3425	90	220.5	235.6	199.2	208.2	117.3	77.2	106.8	106.8	112.1
D1	2109	38	2100	41	101.2	122	64.8	84.5	49.2	-14.4	28.3	18.4	33.8
Y1	2106	38	2100	46	162.9	181.4	132.3	157.9	79.3	21.5	60.4	53.9	66.6
Y2	2502	45	2500	51	177.5	195.2	148.9	161.2	73.5	37.3	74	69.2	71.4

4 conclusions

(1) The water stable isotope indicates that the geothermal water in the Jixian system thermal reservoir in Tongzhou district originates from atmospheric precipitation recharge, and combined with the relationship between the fourth system groundwater recharge-runoff conditions and isotope and hydrochemical characteristics in Tongzhou district, the geothermal water-poor 18O isotope can be interpreted as an elevation effect, and the groundwater recharge elevation formula can calculate the average recharge elevation of geothermal water as 1510m, and the recharge area may be located in the northern and The recharge area may be located in the northern and northwestern mountainous areas of Beijing.

(2) 14C can effectively calculate the age of geothermal water in the thermal reservoir of Jixian system in Tongzhou district. In the west of the study area, the age of geothermal water in the Daxingdian uplift (III7) increases from the northwest (17 ka) to the southeast (28 ka), and the transport rate is about 1.5 m/a. However, in the east of the study area, the transport rate of groundwater accelerates on the Xia mat fracture at the junction of the Daxingdian uplift (III7) and the Dafangxin fault (III8), and the apparent age of groundwater near the fracture becomes lighter.

(3) Sr2+ content and Sr isotopes can effectively trace the flow path of geothermal water and the degree of water-rock interaction in the Jixian system thermal reservoir in Tongzhou District. In the region, the Sr2+ content in geothermal water increases and the n(87Sr)/n(86Sr) values increase as the age of geothermal water increases along the runoff path. Strontium isotopes in geothermal water can be regarded as the superposition of two processes: dissolution of strontium in the Jixian carbonate rocks and decay of87Rb, the latter showing an obvious time-accumulation effect.

(4) K+/Mg2+ cation geothermometer and SiO2 geothermometer without vapor loss can reasonably estimate the thermal storage temperature. In the eastern part of the study area, the average value of thermal storage temperature of two geothermal wells

on the junction of the Daxingdian uplift (Ⅲ7) and the Dazhanxin fault trap (Ⅲ8) reached 107.8℃. In the western part of the study area, the average temperature of thermal storage in the Daxingdian uplift (III7) is 68.3° C, and there is a characteristic of increasing thermal storage temperature with the direction of groundwater runoff.

References

Aas Wenche, Shao Min, Jin Lei, Larssen Thorjorn, Zhao Dawei, Xiang Renjun, Zhang Jinhong, Xiao Jinsong, Duan Lei. 2007. Air concentrations and wet deposition of major inorganic ions at five nonurbansites in China, 2001–2003. Atmospheric Environment, 41:1706 ~ 1716.

Beijing Bureau of Geology and Mineral Resources. 1982#. Regional geology of Beijing. Beijing: Geological Publishing House: 1 ~ 598.

Beijing Bureau of Geology and Mineral Exploration and Development, Beijing Institute of Hydrogeology and Engineering Geology. 2008#. Beijing groundwater. Beijing: China Earth Press: 1 ~ 368.

Clark Ian, Fritz Peter. 1997. Environmental isotopes in hydrology. New York: Lewis Publishers.

Deng Wenping, Yu Xinxiao, Jia Gguodong, Li Yajun, Liu Yujie. 2013. An analysis of characteristics of hydrogen and oxygen stable isotopes in Jiufeng Mountain areas of Beijing. Advances in Water Science, 24(5): 642 ~ 650.

Fournier, RO. 1997. Chemical geothermometers and mixing models for geothermal systems. Geothermics, 5: 41 ~ 50.

Gaillardet J, Dupre B, Louvat P, Allegre CJ. 1999. Global silicate-weathering and CO_2 consumption rates deduced from the chemistry of large rivers. Chemical Geology, 159(1): 3 ~ 30.

Guo Yonghai, Shen Zhaoli, Zhong Zuoshen. 2002&. Hydrogeochemical modeling for the formation of deep-lying alkaline fresh groundwater in Heibei Plain : a case study in Baoding and Cangzhou districts. Earth Science, 27(02): 157 ~ 162.

Kong Xiangjun. 2019&. Discussion on microscopic features of geothermal reservoirs from Wumishan formation in Tongzhou of Beijing. Urban Geology, 14(04): 30 ~ 36.

Li Jie, Pang Zhonghe, Kong Yanlong, Wang Shufang, Bai Guoying, Zhao Hongyi, Zhou Dong, Sun Feng, Yang Zhongshan. 2018 Groundwater isotopes biased toward heavy rainfall events and implications on the Local Meteoric Water Line. Journal of Geophysical Research: Atmospheres, 123: 6259 ~ 6266.

Liu Jianrong, Song Xianfang, Yuan Guofu, Sun Xiaomin, Liu Xin, Wang Shiqin. 2009. Characteristics of $\delta^{18}O$ in precipitation over Eastern Monsoon China and the water vapor sources. Chinese Science Bulletion, 55(2): 200 ~ 211.

Liu Kai, Wang Shanshan, Sun Yin, Cui Wenjun, Zhu Deli. 2017&. Characteristics and regionalization of geothermal resources in Beijing. Geoglogy In China, 44(06): 1128 ~ 1139.

Ma Zhiyuan, Fang Jijiao. 2005&. Sulphate forming from groundwater in eastern Weibei karst area, Shaanxi Province. Coal Geology & Exploration, 33(3): 45 ~ 52.

Min Maozhong, Peng Xinjian, Zhou Xianlin, Qiao Haiming, Wang Jinping, Zhang Li. 2007. Hydrochemistry and isotope compositions of groundwater from the Shihongtan sandstone-hosted uranium deposit, Xinjiang, NW China. Journal of Geochemical Exploration, 93(2): 91 ~ 108.

Pearson FJ. 1965. Use of $^{13}C/^{12}C$ ratios to correct radiocarbon ages of material initially diluted by limestone. In: Proceeding of the 6th International Conference on Radiocarbon and Tritium Dating, Pulman, Washington, 357.

Negrel Philippe. 2006. Water-granite interaction: clues from strontium, neodymium and rare earth elements in soil and waters. Applied Geochemistry, 21: 1432 ~ 1454.

Shand P, Darbyshire PF, Love AJ, Edmunds WM. 2009. Sr isotopes in natural waters: Applications to source characterization and water -rock interaction incontrasting landscapes. Applied Chemistry, 24(4): 574 ~ 586.

Xu Zhifang, Han Guilin. 2009. Chemical and strontium isotope characterization of rainwater in Beijing, China. Atmospheric Environment, 43(12): 1954 ~ 1961.

Ye Ping, Jin Qinshen, Zhou Aaiguo, Liu Cunfu, Cai Hesheng, Gan Yiqun. 2008&. Formation Mechanism of Sr Isotopes in Groundwater of Hebei Plain. Earth Science-Journal of China University of Geosciences, 33(01): 137 ~ 144.

Yu Yuan. 2006&. A study of hydrochemistry and isotopes in thermal groundwater in the urban

geothermal fileld, Beijing. Dissertation Supervisor: Zhou Xun. Beijing: China University of Geosciences(Beijing) Master's Thesis: 1 ~ 67.

Yuan Lijuan, Kong Xiangjun, Gao Jian, Sheng Pengfei, He Yuncheng, Feng Hao, Li Wen, Hao Weijun. 2020&. Genetic model of the Yanqing geothermal field, Beijing. Geoglogical Review, 66(04): 933 ~ 941.

Zhai Yuanzheng, Wang Jinsheng, Zuo Rui, Teng Yanguo. 2011&. Strontium Isotopic Tracing of Water-Rock Interaction in Quaternary Aquifer in Beijing Plain. Science & Technology Review, 29(06): 17 ~ 20.

Zhang Jinping, Yuan Lijuan. 2018&. Effection of Xiadian fault on geothermal resource distribution— A case study in Xiji District. Urban Geology, 13(03): 15 ~ 20.

Zou Deng Liang, Zhang Jinping, Yuan Lijuan, Zhang Qinrui, Shi Hanjing. 2015#. First discovery of medium-temperature geothermal resources in Tongzhou District, Beijing. Urban Geology, 10(04): 52.